Systematic analysis of the proton mass radius based on photoproduction of vector charmoniums

Xiao-Yun Wang,[1,2,*] Fancong Zeng,[1,†] and Quanjin Wang[1]

[1]*Department of physics, Lanzhou University of Technology, Lanzhou 730050, China*
[2]*Lanzhou Center for Theoretical Physics, Key Laboratory of Theoretical Physics of Gansu Province, Lanzhou University, Lanzhou, Gansu 730000, China*

(Received 18 April 2022; accepted 13 May 2022; published 27 May 2022)

In this work, the cross section of the reaction $\gamma p \to V(J/\psi, \psi(2S))p$ from the production threshold to medium energy is studied and systematically analyzed within two gluon exchange model. The obtained numerical results are in agreement with experimental data and other theoretical predictions. Under the assumption of the scalar form factor of dipole form, the value of proton mass radius is calculated as 0.55 ± 0.09 fm and 0.77 ± 0.12 fm from the fit to the predicted J/ψ and $\psi(2S)$ differential cross section, respectively. Finally, the average value of proton mass radius is estimated to be $\sqrt{\langle R_m^2 \rangle} = 0.67 \pm 0.11$ fm. Moreover, one finds that extracting mass radius from the near-threshold differential cross section of heavy quarkoniums is always affected by large $|t|_{\min}$. These obtained results may provide important theoretical reference for the understanding of nucleon structure and future relevant experiments.

DOI: 10.1103/PhysRevD.105.096033

I. INTRODUCTION

The proton radius is a big inspiration in understanding the proton structure, and it can be measured by using the lepton as probe. Usually, the proton radius can be estimated by colliding the nucleus with high-energy electrons and observing the angles and energies of these electrons scattered from the nucleus. In the past decade, several groups have given their results [1–10] and the latest values of the proton charge and magnetic radius are calculated as 0.8409 fm [11] and 0.817 fm [12], respectively. In fact, it is theoretically possible to use graviton as a probe to determine the proton radius, which is usually called proton mass radius. Since the interaction of gravitons and proton scattering is very weak, far beyond the measurement limit of current experiments, it is difficult to directly measure the proton mass radius experimentally. In recent study, the mass radius is described by the scalar gravitational form factors (GFFs) of the energy momentum tensor trace of quantum chromodynamics (QCD) [13–15]. Under the framework of QCD theory, the photoproduction of a quarkonium off the proton is connected to GFFs of the proton, which is sensitive to the proton mass distribution from the quantum chromodynamics trace anomaly [15,16]. Under an assumption of the scalar form factor of dipole form, the proton mass radius can be extracted via the near-threshold photoproduction data of vector quarkoniums [17,18].

In recent years, researchers have made relevant calculations and studies on the proton mass radius using vector meson photoproduction data. In Ref. [19], the gluonic contributions to the quantum anomalous energy, mass radius, spin, and mechanical pressure in the proton are studied by analyzing the near-threshold production of heavy quarkonium, and the proton mass radius is calculated as 0.68 fm. By studying the near-threshold differential cross section of the vector mesons, one work [20] gives the average value of mass radius as 0.67 ± 0.03 fm, according to ω, ϕ, J/ψ experimental data [21–23]. Kharzeev calculates that the mass radius is 0.55 ± 0.03 fm [17] according to GlueX data of J/ψ photoproduction [23]. One notices that the proton's mass radius is smaller than its charge radius, which may mean that the mass distribution of protons is tighter than the charge distribution, and different interaction forces correspond to different proton radius.

In the charm quark energy region, due to the mass of J/ψ and $\psi(2S)$ both being below the mass threshold of $D\bar{D}$, hadron decay via Okubo-Zweig-Izuki (OZI) suppression makes their decay widths very small. The small decay widths give J/ψ and $\psi(2S)$ a long life, which is beneficial to observe the relevant physical quantities in the experiment. Therefore, it is of great interest to systematically analyze the proton mass radius from photoproduction of vector

*Corresponding author.
xywang@lut.edu.cn
†fczeng@yeah.net

charmoniums. Currently, the photoproduction of J/ψ has been measured with an increasing precision over a large energy range [23–31], while the measurements of $\psi(2S)$ photoproduction data are very meagre (only some sparse data exist near 100 GeV) [32–34]. Among them, although GlueX [23] measured the near-threshold photoproduction differential cross section of J/ψ, the corresponding center-of-mass energy was 4.58 GeV, which was several hundred mega-electron-volts larger than the threshold energy. For $\psi(2S)$, photoproduction differential cross-section data at threshold are not yet available. Such a situation results in that we can only rely on limited experimental data when extracting the proton mass radius, and it is difficult to systematically analyze and describe the overall influence of the cross section near the threshold of the vector charmoniums on the proton mass radius. Therefore, one need to first consider the theoretical calculation and prediction of charmoniums [J/ψ and $\psi(2S)$] photoproduction with the help of physical models, and then systematically study the mass radius based on the theoretical differential cross section.

Considering the $\psi(2S)$ and J/ψ have close mass and the same quantum number, it is reasonable to study them with the same physical model and parameters. Since the two-gluon exchanging process may predominate in charmonium photoproduction [34,35], in this work we attempt to extend the study of J/ψ to $\psi(2S)$ under the framework of the two gluon exchange model, providing data for the systematic extraction of proton mass radius. The paper is organized as follows. The formulas of the two gluon exchange model and the relation between mass radius and differential cross section are provided in Sec. II. Then in Sec. III, we show the numerical result on the explanations of the current experimental data of J/ψ photoproduction, the predictions of $\psi(2S)$ photoproduction, and the discussion and results of mass radius $\sqrt{\langle R_m^2 \rangle}$. A short summary is given in Sec. IV.

II. FORMALISM

A. Two gluon exchange model

The two gluon exchange model is based on the photon fluctuation into the quark-antiquark pair ($\gamma \to c + \bar{c}$) and the double gluon exchange between the nucleon state and the quark-antiquark pair. Here, the $c\bar{c}$ fluctuation of the photon treated as a color dipole. Finally, the dipole forms into final vector meson. The picture of the double gluon exchange is illustrated in Fig. 1. Here, we describe the process

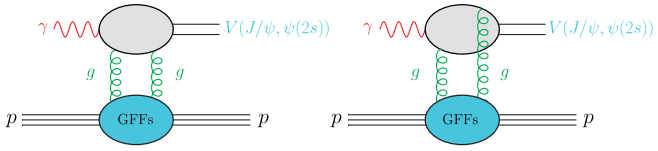

FIG. 1. The schematic Feynman diagram of the two-gluon exchange for $V(J/\psi, \psi(2S))$ production.

$$\gamma(q) + p(p) \to V(q_1) + p(p_1), \tag{1}$$

where $V = J/\psi, \psi(2S)$.

Because of the hard scale in the heavy quarkonium production, the exclusive vector meson photoproduction amplitude is given by [36–38]

$$\mathcal{T} = \frac{i\sqrt{2}\pi^2}{3} m_q \alpha_s e_q f_V F_{2g}(t) \times \left[\frac{xg(x, Q_0^2)}{m_q^4} + \int_{Q_0^2}^{+\infty} \frac{dl^2}{m_q^2(m_q^2 + l^2)} \frac{\partial xg(x, l^2)}{\partial l^2} \right]. \tag{2}$$

The amplitude is normalized and $\frac{d\sigma}{dt} = \alpha|\mathcal{T}|^2$. The J/ψ and $\psi(2S)$ photoproduction differential cross section at low momentum transfer are purely diffractive and given as [35,39]

$$\frac{d\sigma}{dt} = \frac{\pi^3 \Gamma^V_{e^+e^-} \alpha_s}{6\alpha m_q^5} [xg(x, m_V^2)]^2 \exp(bt), \tag{3}$$

where $x = m_V^2/W^2$, W is the center-of-mass energy of the γp collision; t is the momentum transfer. $\alpha_s = 0.5$ is the strong running coupling constant [40], $\alpha = 1/137$ is the electromagnetic coupling constant, $m_q = 1.27$ GeV is the mass of c quark. $\Gamma^V_{e^+e^-}$ is the radiative decay of vector meson. In this paper, we set $\Gamma^{J/\psi}_{e^+e^-} = 5.547$ keV and $\Gamma^{\psi(2S)}_{e^+e^-} = 2.33$ keV from Particle Data Group [41]. The factor $xg(x, m_V^2)$ is the gluon distribution function at $Q^2 = m_V^2$, which is parametrized using a simple function form $xg(x, m_V^2) = A_0 x^{A_1}(1-x)^{A_2}$ [42]. In this paper, the photoproduction of J/ψ and $\psi(2S)$ will use the same gluon distribution function.

The last exponential factor in Eq. (3) usually describes the differential cross section of vector meson at low momentum transfer. The exponential slope b for J/ψ has little variance with W, which is given as [35]

$$b^{J/\psi}(W) = b_0^{J/\psi} + 0.46 \cdot In(W/W_0^{J/\psi}) \tag{4}$$

and fixed the slope $b_0^{J/\psi} = 1.67 \pm 0.38$ GeV^{-2} at the energy $W_0^{J/\psi} = 4.58$ GeV [23]. For $b^{\psi(2S)}(W)$, we use the standard form based on the Regge phenomenology [34,43]

$$b^{\psi(2S)}(W) = b_0^{\psi(2S)} + 4\alpha'(0) In(W/W_0), \qquad W_0 = 90 \text{ GeV} \tag{5}$$

the parameters have been determined from a fit to HERA data that $b_0^{\psi(2S)} = 4.86$ and $\alpha'(0) = 0.151$ [34].

The total cross section is obtained by integrating the differential cross section [Eq. (3)] over the allowed kinematical range from $t_{\min}$ to $t_{\max}$, which can be written as

$$\sigma = \int_{t_{\min}}^{t_{\max}} dt \left(\frac{d\sigma}{dt}\right). \quad (6)$$

Here, the limiting values $t_{\min}$ and $t_{\max}$ are

$$t_{\max}(t_{\min}) = \left[\frac{m_1^2 - m_3^2 - m_2^2 + m_4^2}{2W}\right]^2 - (p_{1\,\mathrm{cm}} \mp p_{3\,\mathrm{cm}})^2. \quad (7)$$

The center-of-mass energies and momenta of the incoming photon and vector meson are

$$p_{i\mathrm{cm}} = \sqrt{E_{i\mathrm{cm}}^2 - m_i^2} \quad (i = 1, 3), \quad (8)$$

$$E_{1\,\mathrm{cm}} = \frac{W^2 + m_1^2 - m_2^2}{2W}, \text{ and } E_{3\,\mathrm{cm}} = \frac{W^2 + m_3^2 - m_4^2}{2W}. \quad (9)$$

In addition, one notices that in Refs. [44–46], the real part of the $J/\psi - p$ scattering amplitude is of great success in vector meson photoproduction around the threshold, which indicates that the real part of the scattering amplitude is in general important at low energies. Considering the trace terms in the OPE can no longer be neglected at low energies, more theoretical research on the two gluon exchange model and related physical mechanisms is still needed.

B. GFFs and mass radius

The mass radius can be defined in terms of the scalar gravitational form factors $G(t)$; the definition of the mass radius is given by [17,47]

$$\langle R_m^2 \rangle \equiv \frac{6}{M} \frac{dG(t)}{dt}\bigg|_{t=0} \quad (10)$$

with $G(0) = M$. And the scalar gravitational form factor is defined as

$$G(t) = \frac{M}{(1 - t/m_s^2)^2}, \quad (11)$$

in which m_s is a free parameter. According to the definition, the mass radius is connected to the dipole parameter m_s as

$$\langle R_m^2 \rangle = \frac{12}{m_s^2}. \quad (12)$$

The differential cross section of the photoproduction of the quarkonium can be described with the GFFs, which is written as [17,48–50]

$$\frac{d\sigma}{dt} \propto G^2(t). \quad (13)$$

Therefore, it is an effective way to extract proton mass radius by learning the near-threshold photoproduction data of charmoniums.

TABLE I. The fitted values of the parameters A_0, A_1, A_2 describing the gluon distribution function $xg(x)$ according to J/ψ photoproduction. and the reduced χ^2/d.o.f.

A_0	A_1	A_2	χ^2/d.o.f.
0.228 ± 0.045	-0.218 ± 0.006	1.221 ± 0.055	2.066

III. RESULTS AND DISCUSSION

A. Cross section of charmoniums photoproduction

The parametrization gluon distribution function $xg(x, m_V^2) = A_0 x^{A_1}(1-x)^{A_2}$ is introduced and used in two gluon exchange model discussed in the above section. The free parameters A_0, A_1, and A_2 then are fixed by a global analysis of both the total cross-section data below medium energy (center of mass (c.m.) energy near 400 GeV) [23–30] and the near-threshold ($W = 4.58$ GeV) differential cross-section data [23] of J/ψ. The obtained parameters of gluon distribution are listed in Table I. The total cross section of $\gamma p \to J/\psi p$ as a function of c.m. energy W is shown in Fig. 2, compared to several experimental data [23–31]. The comparison between the differential cross section and the experimental measurements is manifested in Fig. 3, exhibiting a good agreement. Finally, one notices that the χ^2/d.o.f. of our global fit is calculated to be 2.066, which indicates that the parameters obtained from gluon distribution is applicable for J/ψ photoproduction.

Using the parameters in Table I, one calculates the photoproduction cross section of $\psi(2S)$, as shown by the blue solid curve in Fig. 4. It is shown that the theoretical calculations are in good agreement with the experimental data [32–34] of $\psi(2S)$ photoproduction. Moreover, the ratio of $\psi(2S)$ to J/ψ total cross section $R = \sigma_{\psi(2S)p}/\sigma_{J/\psi p}$ is

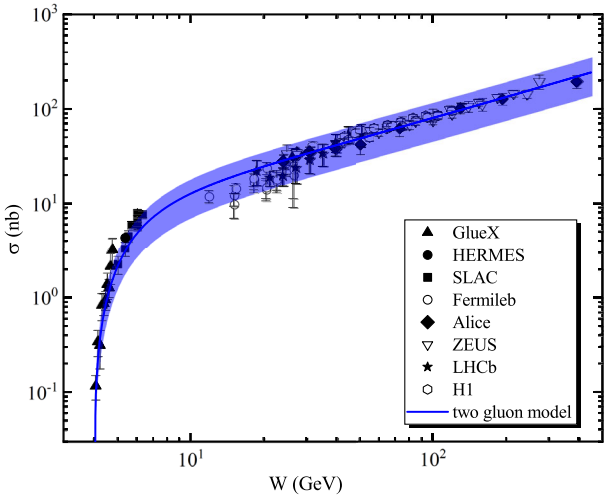

FIG. 2. The total cross section of $\gamma p \to J/\psi p$ as a function of W in two gluon exchange model. The band reflect the error bar of the A_0. References of data can be found in [23–31].

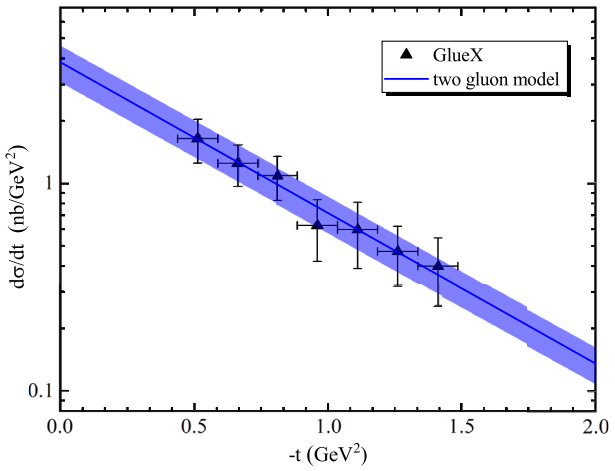

FIG. 3. The differential cross section of $\gamma p \to J/\psi p$ as a function of $-t$ in two gluon exchange model. Reference of data can be found in [23].

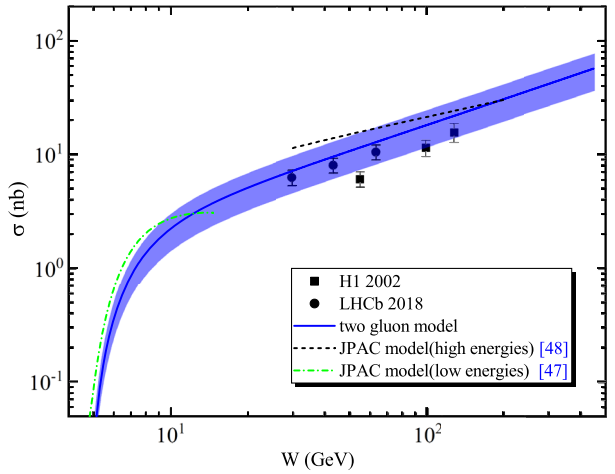

FIG. 4. The total cross section of $\gamma p \to \psi(2S)p$ as a function of W. The blue solid curve is obtained from the two gluon exchange model. Black dotted curve and green dot-dashed curve are obtained from the prediction of JPAC in high energies and low energies, respectively. References of data can be found in [32–34].

estimated as a function of W in Fig. 5, which also agrees well with the experimental data [32]. The above results indicate that it is suitable and feasible to extend the study from J/ψ to $\psi(2S)$ production under the framework of the two gluon exchange model. Moreover, it is worth mentioning that two effective Pomeron models are considered to research the $\psi(2S)$ photoproduction in low and high energy regions by Joint Physics Analysis Center (JPAC) [51,52]. We compared our results with JPAC models, which are shown in Figs. 4 and 6. The prediction of JPAC models are basically consistent with our results at the threshold, while it is larger than experimental data in higher energy regions.

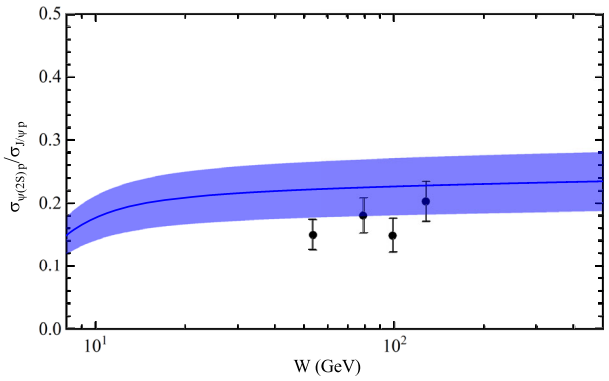

FIG. 5. The result of $J/\psi p$ and $\psi(2S)p$ total cross-section ratio R as a function of W. Reference of data can be found in [32].

B. proton mass radius

Under the assumption of the scalar form factor of dipole form, the proton mass radius can be extracted from the near-threshold differential cross section of vector charmoniums. In this work, the differential cross section of $\gamma p \to \psi(2S)p$ are predicted by two gluon exchange model. We choose the c.m. energy $W \in (4.88, 5.28)$ interval of 0.1 GeV and a range of $\Delta t = 0.5$ GeV^2 starting with $|t|_{\min}$, which are shown in the black squares in Fig. 7. The blue solid curve in Fig. 7 is the fitted scalar gravitational form factor of the dipole parametrization in Eq. (13). Finally, we get the value of proton mass radius from Eqs. (12) and (13), which are the first five blue squares in Fig. 10. Here, the small x axis $(W - W_{\text{thr}})/W_{\text{thr}}$ represents the c.m. energy close to the threshold energy W_{thr}. For J/ψ mesons, the numerical results obtained from similar methods can be seen in Fig. 8 and the first five red circles in Fig. 10.

Note that, the proton mass radius mainly depends on the slope of the vector meson threshold photoproduction cross section, and is hardly affected by the cross-section size. However, one finds that although the slope b at the threshold changes very slowly [which can be verified

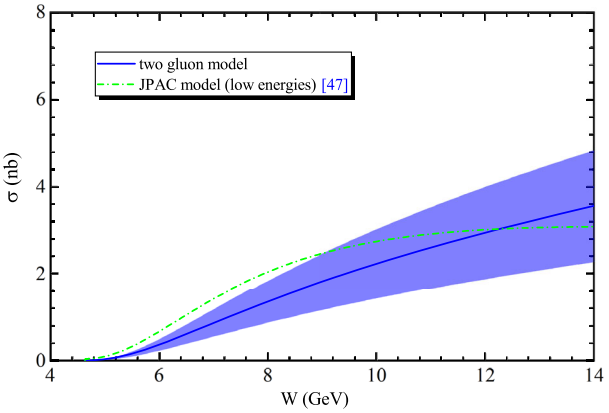

FIG. 6. The total cross section of $\gamma p \to \psi(2S)p$ as a function of W. The curves have the same meaning as in Fig. 4.

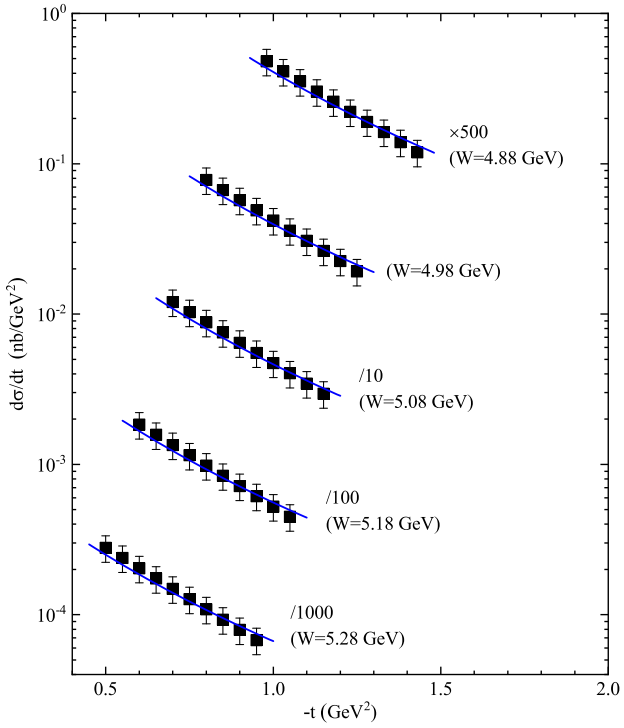

FIG. 7. The differential cross section of $\psi(2S)$ in Eq. (13) is shown in the blue solid curve. Black squares show the predicted differential cross section of $\gamma p \to \psi(2S)p$ as a function of $-t$.

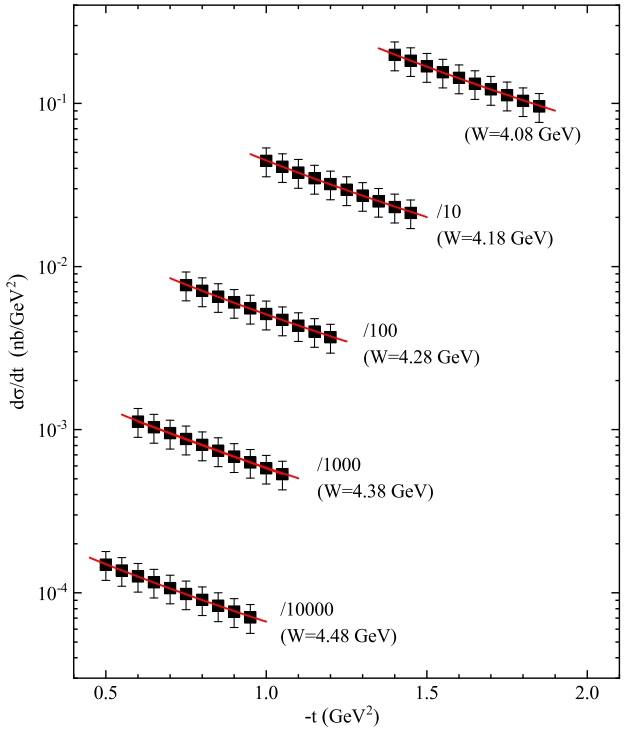

FIG. 8. The differential cross section of J/ψ in Eq. (13) is shown in the red solid curve. Black squares show the predicted differential cross section of $\gamma p \to J/\psi p$ as a function of $-t$.

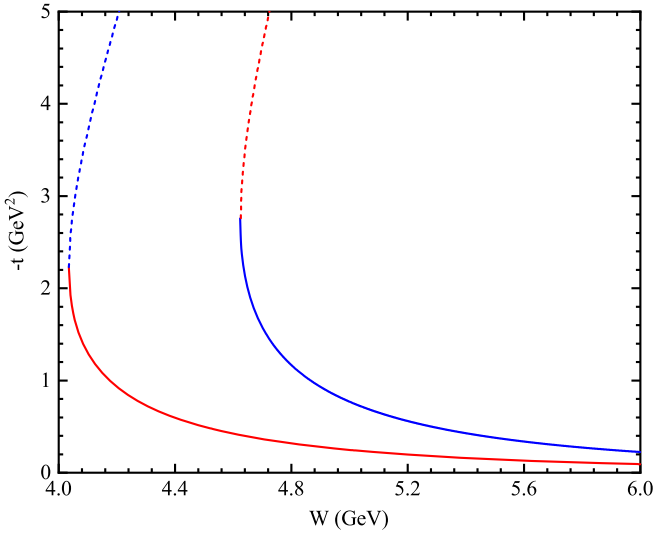

FIG. 9. The limiting values $t_{\min}$ and $t_{\max}$ as a function of W. The blue solid curve shows $|t|_{\min}$ of $\psi(2S)p$ photoproduction. The red solid curve shows $|t|_{\min}$ of $J/\psi p$ photoproduction.

by Eqs. (4) and (5)], the extracted mass radius changes sharply at the threshold, as shown in Fig. 10. Actually, the main reason is that the rapidly varies of $|t|_{\min}$ near threshold. Accordingly, one can give the invariant momentum transfer $|t|$ at the threshold equal to

$$|t|_{\rm thr} = |t|_{\min}(W_{\rm thr}) = |t|_{\max}(W_{\rm thr}) = \frac{M_N M_V^2}{M_N + M_V}. \quad (14)$$

By analyzing the formula, it can be obtained that when the mass of the vector meson is heavier, the corresponding

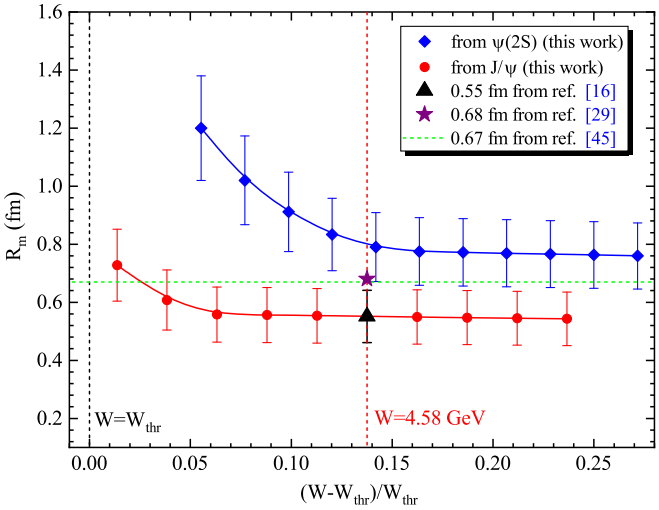

FIG. 10. The extracted mass radius at different c.m. energy from predicted $\psi(2S)$ photoproduction (blue squares) and J/ψ photoproduction (red circles). The green line shows the result of Ref. [20]. The purple pentagram shows the result of Ji [19]. The black triangle shows the result of Kharzeev [17].

$|t|_{\rm thr}$ is also larger, which eventually leads to $|t|_{\rm min}$ having more rapid variation near threshold, as shown in Fig. 9. This indicates that $|t|_{\rm min}$ has a greater effect on the heavier vector mesons. The above situation requires us to pay special attention when extracting the proton mass radius, and to perform overall analysis and extraction to avoid single-point dependence. For some light vector mesons (such as ϕ mesons, etc.) photoproduction, since the change of $|t|_{\rm min}$ at the threshold is relatively gentle, it is beneficial to the experimental measurement of the near-threshold cross section and the extraction of the mass radius.

As shown in Fig. 10, the influence of big $|t|_{\rm min}$ on extracting the mass radius in $\psi(2S)p$ and $J/\psi p$ photoproduction can be eliminated with the increase of c.m. energy. Since the extracted mass radius gradually tends to a stable value with the increase of energy, we consider selecting an energy interval closest to the threshold, and determine the stable value of the mass radius in this energy interval as the required physical quantity. Thus, the average value of dipole parameter $m_s = 0.88 \pm 0.11$ GeV and mass radius is calculated as 0.77 ± 0.12 fm from the $\psi(2S)p$ differential cross section with $W \in (5.28, 5.88)$. The mass radius is calculated as 0.55 ± 0.09 fm from $J/\psi p$ photoproduction with $W \in (4.38, 5.98)$. Finally, the average value of the proton mass radius is calculated to be $\sqrt{\langle R_m^2 \rangle} = 0.67 \pm 0.11$ fm.

By studying the near-threshold differential cross section of the vector mesons ω, ϕ, J/ψ, one work [20] gets the average value of the proton mass radius as 0.67 ± 0.03 fm (the green dotted curve in Fig. 10). Kharzeev calculates the mass radius 0.55 ± 0.03 fm (the black triangle in Fig. 10) [17] according to GlueX data of J/ψ photoproduction [23], while Ji calculates that the proton mass radius is 0.68 fm (the purple pentagram Fig. 10) [19]. In fact, if the error bar is considered, our results are in agreement with the above theoretical predictions.

IV. SUMMARY

We have reproduced the total and differential cross section of the reaction $\gamma p \to J/\psi p$ from the production threshold to medium energy (W near 400 GeV) with the two gluon exchange model encountering a parametrized gluon distribution function. By fitting the experimental data, one get the parameters of the gluon distribution function and the result shows that the two gluon exchange model depicts well both the differential and total cross section of J/ψ in a wide energy range. Subsequently, one estimates the photoproduction of the $\psi(2S)$ meson using the gluon distribution determined by J/ψ photoproduction. The comparison between our theoretical prediction and $\psi(2S)$ experimental data is good. Naturally, the proton mass radius is extracted by using the predicted differential cross section of charmoniums [J/ψ and $\psi(2S)$]. After system analysis, the average value of the proton mass radius is estimated to be 0.67 ± 0.11 fm. This value is smaller than proton charge and magnetic radius, but is basically close to the mass radius value given by other theoretical groups [17,19,20]. We also find that extracting the mass radius from the near-threshold differential cross section is always affected by large $|t|_{\rm min}$. This requires us to take special care in extracting mass radius through the near-threshold cross section of heavy vector quarkoniums photoproduction. Of course, more accurate experimental measurement data for the photo- and electroproduction of charmoniums is still needed, which can be realized not only in the JLab experiment [23], but also within the capabilities of Electron-ion collider in China and Electron-ion collider in U.S. facility [53,54]. Moreover, the results of charmoniums photoproduction will provide an important theoretical reference for ultraperipheral collisions (UPCs) [55–58]. Therefore, it would also be interesting to investigate the production of charmoniums in ep and pA collisions according to the actual situation of EIC and UPCs experiments.

ACKNOWLEDGMENTS

X.-Y. Wang would like to acknowledge Dr. Daniel Winney for useful discussion about the JPAC model. This project is supported by the National Natural Science Foundation of China (Grants No. 12065014 and No. 12047501), and by the West Light Foundation of The Chinese Academy of Sciences, Grant No. 21JR7RA201.

[1] R. Pohl, A. Antognini, F. Nez, F. D. Amaro, F. Biraben, J. M. R. Cardoso, D. S. Covita, A. Dax, S. Dhawan, L. M. P. Fernandes *et al.*, The size of the proton, Nature (London) **466**, 213 (2010).

[2] J. C. Bernauer *et al.* (A1 Collaboration), High-Precision Determination of the Electric and Magnetic Form Factors of the Proton, Phys. Rev. Lett. **105**, 242001 (2010).

[3] A. Antognini, F. Nez, K. Schuhmann, F. D. Amaro, François Biraben, J. M. R. Cardoso, D. S. Covita, A. Dax, S. Dhawan, M. Diepold *et al.*, Proton structure from the measurement of $2S - 2P$ transition frequencies of muonic hydrogen, Science **339**, 417 (2013).

[4] J. M. Alarcón, D. W. Higinbotham, C. Weiss, and Z. Ye, Proton charge radius extraction from electron scattering data

using dispersively improved chiral effective field theory, Phys. Rev. C **99**, 044303 (2019).
[5] A. Beyer, L. Maisenbacher, A. Matveev, R. Pohl, K. Khabarova, A. Grinin, T. Lamour, D. C. Yost, T. W. Hänsch, N. Kolachevsky, and T. Udem, The Rydberg constant and proton size from atomic hydrogen, Science **358**, 79 (2017).
[6] N. Bezginov, T. Valdez, M. Horbatsch, A. Marsman, A. C. Vutha, and E. A. Hessels, A measurement of the atomic hydrogen Lamb shift and the proton charge radius, Science **365**, 1007 (2019).
[7] H. Fleurbaey, S. Galtier, S. Thomas, M. Bonnaud, L. Julien, F. Biraben, F. Nez, M. Abgrall, and J. Guéna, New Measurement of the $1S-3S$ Transition Frequency of Hydrogen: Contribution to the Proton Charge Radius Puzzle, Phys. Rev. Lett. **120**, 183001 (2018).
[8] M. Mihovilovič, P. Achenbach, T. Beranek, J. Beričič, J. C. Bernauer, R. Böhm, D. Bosnar, M. Cardinali, L. Correa, L. Debenjak *et al.*, The proton charge radius extracted from the initial-state radiation experiment at MAMI, Eur. Phys. J. A **57**, 107 (2021).
[9] W. Xiong, A. Gasparian, H. Gao, D. Dutta, M. Khandaker, N. Liyanage, E. Pasyuk, C. Peng, X. Bai, L. Ye *et al.*, A small proton charge radius from an electron–proton scattering experiment, Nature (London) **575**, 147 (2019).
[10] X. Zhan, K. Allada, D. S. Armstrong, J. Arrington, W. Bertozzi, W. Boeglin, J. P. Chen, K. Chirapatpimol, S. Choi, E. Chudakov *et al.*, High-precision measurement of the proton elastic form factor ratio $\mu_p G_E/G_M$ at low Q^2, Phys. Lett. B **705**, 59 (2011).
[11] P. A. Zyla *et al.* (Particle Data Group), Review of particle physics, Prog. Theor. Exp. Phys. **2020**, 083C01 (2020).
[12] Z. F. Cui, D. Binosi, C. D. Roberts, and S. M. Schmidt, Pauli radius of the proton, Chin. Phys. Lett. **38**, 121401 (2021).
[13] I. Y. Kobzarev and L. B. Okun, Gravitational interaction of fermions, Zh. Eksp. Teor. Fiz. **43**, 1904 (1962), https://inspirehep.net/literature?sort=mostrecent&size=25&page=1&q=Kobzarev%3A1962wt&ui-citation-summary=true.
[14] H. Pagels, Energy-momentum structure form factors of particles, Phys. Rev. **144**, 1250 (1966).
[15] X. D. Ji, Deeply virtual Compton scattering, Phys. Rev. D **55**, 7114 (1997).
[16] R. Wang, J. Evslin, and X. Chen, The origin of proton mass from J/Ψ photo-production data, Eur. Phys. J. C **80**, 507 (2020).
[17] D. E. Kharzeev, Mass radius of the proton, Phys. Rev. D **104**, 054015 (2021).
[18] H. Fujii and D. Kharzeev, Long range forces of QCD, Phys. Rev. D **60**, 114039 (1999).
[19] Y. Guo, X. Ji, and Y. Liu, QCD Analysis of near-threshold photon-proton production of heavy quarkonium, Phys. Rev. D **103**, 096010 (2021).
[20] R. Wang, W. Kou, Y. P. Xie, and X. Chen, Extraction of the proton mass radius from the vector meson photoproductions near thresholds, Phys. Rev. D **103**, L091501 (2021).
[21] T. Mibe *et al.* (LEPS Collaboration), Diffractive ϕ-Meson Photoproduction on Proton Near Threshold, Phys. Rev. Lett. **95**, 182001 (2005).
[22] J. Barth, W. Braun, J. Ernst, K. H. Glander, J. Hannappel, N. Jopen, H. Kalinowsky, F. J. Klein, F. Klein, E. Klempt *et al.*, Low-energy of photoproduciton of omega-mesons, Eur. Phys. J. A **18**, 117 (2003).
[23] A. Ali *et al.* (GlueX Collaboration), First Measurement of Near-Threshold J/ψ Exclusive Photoproduction off the Proton, Phys. Rev. Lett. **123**, 072001 (2019).
[24] S. Chekanov *et al.* (ZEUS Collaboration), Exclusive photoproduction of J/ψ mesons at HERA, Eur. Phys. J. C **24**, 345 (2002).
[25] M. E. Binkley, C. Bohler, J. Butler, J. P. Cumalat, I. Gaines, M. Gormley, D. Harding, R. L. Loveless, J. Peoples, P. Callahan *et al.*, J/ψ Photoproduction from 60 to 300 GeV/c, Phys. Rev. Lett. **48**, 73 (1982).
[26] P. L. Frabetti *et al.* (E687 Collaboration), A measurement of elastic J/ψ photoproduction cross-section at fermilab E687, Phys. Lett. B **316**, 197 (1993).
[27] C. Alexa *et al.* (H1 Collaboration), Elastic and proton-dissociative photoproduction of J/ψ mesons at HERA, Eur. Phys. J. C **73**, 2466 (2013).
[28] B. B. Abelev *et al.* (ALICE Collaboration), Exclusive J/ψ Photoproduction off Protons in Ultra-Peripheral p-Pb Collisions at $\sqrt{s_{\mathrm{NN}}} = 5.02$ TeV, Phys. Rev. Lett. **113**, 232504 (2014).
[29] R. Aaij *et al.* (LHCb Collaboration), Exclusive J/ψ and $\psi(2\mathrm{S})$ production in pp collisions at $\sqrt{s} = 7$ TeV, J. Phys. G **40**, 045001 (2013).
[30] S. Acharya *et al.* (ALICE Collaboration), Energy dependence of exclusive J/ψ photoproduction off protons in ultra-peripheral p-Pb collisions at $\sqrt{s_{NN}} = 5.02$ TeV, Eur. Phys. J. C **79**, 402 (2019).
[31] M. J. Amarian, Strangeness and charm production with HERMES, Few-Body Syst. Suppl. **11**, 359 (1999).
[32] C. Adloff *et al.* (H1 Collaboration), Diffractive photoproduction of $\psi(2S)$ mesons at HERA, Phys. Lett. B **541**, 251 (2002).
[33] R. Aaij *et al.* (LHCb Collaboration), Central exclusive production of J/ψ and $\psi(2S)$ mesons in pp collisions at $\sqrt{s} = 13$ TeV, J. High Energy Phys. 10 (2018) 167.
[34] M. Hentschinski and E. Padrón Molina, Exclusive J/Ψ and $\Psi(2s)$ photo-production as a probe of QCD low x evolution equations, Phys. Rev. D **103**, 074008 (2021).
[35] F. Zeng, X. Y. Wang, L. Zhang, Y. P. Xie, R. Wang, and X. Chen, Near-threshold photoproduction of J/ψ in two-gluon exchange model, Eur. Phys. J. C **80**, 1027 (2020).
[36] M. G. Ryskin, Diffractive J/ψ electroproduction in LLA QCD, Z. Phys. C **57**, 89 (1993).
[37] S. J. Brodsky, L. Frankfurt, J. F. Gunion, A. H. Mueller, and M. Strikman, Diffractive leptoproduction of vector mesons in QCD, Phys. Rev. D **50**, 3134 (1994).
[38] M. G. Ryskin, R. G. Roberts, A. D. Martin, and E. M. Levin, Diffractive J/ψ photoproduction as a probe of the gluon density, Z. Phys. C **76**, 231 (1997).
[39] A. Sibirtsev, S. Krewald, and A. W. Thomas, Systematic analysis of charmonium photoproduction, J. Phys. G **30**, 1427 (2004).
[40] Y. Xu, Y. Xie, R. Wang, and X. Chen, Estimation of $\Upsilon(1\mathrm{S})$ production in ep process near threshold, Eur. Phys. J. C **80**, 283 (2020).

[41] M. Tanabashi *et al.* (Particle Data Group), Review of particle physics, Phys. Rev. D **98**, 030001 (2018).
[42] J. Pumplin, D. R. Stump, J. Huston, H. L. Lai, P. M. Nadolsky, and W. K. Tung, New generation of parton distributions with uncertainties from global QCD analysis, J. High Energy Phys. 07 (2002) 012.
[43] J. Cepila, J. Nemchik, M. Krelina, and R. Pasechnik, Theoretical uncertainties in exclusive electroproduction of S-wave heavy quarkonia, Eur. Phys. J. C **79**, 495 (2019).
[44] D. Kharzeev, H. Satz, A. Syamtomov, and G. Zinovjev, J/ψ photoproduction and the gluon structure of the nucleon, Eur. Phys. J. C **9**, 459 (1999).
[45] D. Kharzeev, Quarkonium interactions in QCD, Proc. Int. Sch. Phys. Fermi **130**, 105 (1996), https://inspirehep.net/literature?sort=mostrecent&size=25&page=1&q=arXiv%3Anucl-th%2F9601029&ui-citation-summary=true.
[46] O. Gryniuk and M. Vanderhaeghen, Accessing the real part of the forward $J/\psi - p$ scattering amplitude from J/ψ photoproduction on protons around threshold, Phys. Rev. D **94**, 074001 (2016).
[47] G. A. Miller, Defining the proton radius: A unified treatment, Phys. Rev. C **99**, 035202 (2019).
[48] K. A. Mamo and I. Zahed, Diffractive photoproduction of J/ψ and Υ using holographic QCD: Gravitational form factors and GPD of gluons in the proton, Phys. Rev. D **101**, 086003 (2020).
[49] Y. Hatta, A. Rajan, and D. L. Yang, Near threshold J/ψ and Υ photoproduction at JLab and RHIC, Phys. Rev. D **100**, 014032 (2019).
[50] L. Frankfurt and M. Strikman, Two gluon form-factor of the nucleon and J/ψ photoproduction, Phys. Rev. D **66**, 031502 (2002).
[51] D. Winney, C. Fanelli, A. Pilloni, A. N. Hiller Blin, C. Fernández-Ramírez, M. Albaladejo, V. Mathieu, V. I. Mokeev, and A.P. Szczepaniak (JPAC Collaboration), Double polarization observables in pentaquark photoproduction, Phys. Rev. D **100**, 034019 (2019).
[52] M. Albaladejo, A. N. Hiller Blin, A. Pilloni, D. Winney, C. Fernández-Ramírez, V. Mathieu, and A. Szczepaniak (JPAC Collaboration), XYZ spectroscopy at electron-hadron facilities: Exclusive processes, Phys. Rev. D **102**, 114010 (2020).
[53] A. Accardi, J. L. Albacete, M. Anselmino, N. Armesto, E. C. Aschenauer, A. Bacchetta, D. Boer, W. K. Brooks, T. Burton, N. B. Chang *et al.*, Electron Ion Collider: The next QCD frontier: Understanding the glue that binds us all, Eur. Phys. J. A **52**, 268 (2016).
[54] D. P. Anderle, V. Bertone, X. Cao, L. Chang, N. Chang, G. Chen, X. Chen, Z. Chen, Z. Cui, L. Dai *et al.*, Electron-ion collider in China, Front. Phys. (Beijing) **16**, 64701 (2021).
[55] S. R. Klein, J. Nystrand, J. Seger, Y. Gorbunov, and J. Butterworth, STARlight: A Monte Carlo simulation program for ultra-peripheral collisions of relativistic ions, Comput. Phys. Commun. **212**, 258 (2017).
[56] S. R. Klein and Y. P. Xie, Photoproduction of charged final states in ultraperipheral collisions and electroproduction at an electron-ion collider, Phys. Rev. C **100**, 024620 (2019).
[57] X. Y. Wang, W. Kou, Q. Y. Lin, Y. P. Xie, X. Chen, and A. Guskov, Production of the bottomonium-like states Z_b states at $e - h$ and ultraperipheral $h - h$ collisions, Chin. Phys. C **45**, 5 (2021).
[58] Y. P. Xie, X. Y. Wang, and X. Chen, Production of vector mesons in pentaquark state resonance channel in $p - A$ ultraperipheral collisions, Chin. Phys. C **45**, 014107 (2021).